Stereodynamics study of reactions $N(^2D)+HD\rightarrow NH+D$ and $ND+H^*$

Yue Xian-Fang(岳现房)[a)†], Cheng Jie(程 杰)[a)], Li Hong(李 宏)[a)], Zhang Yong-Qiang(张永强)[a)], and Emilia L. Wu[b)]

[a)] *Department of Physics and Information Engineering, Jining University, Qufu* 273155, *China*

[b)] *Department of Chemical Engineering and Materials Science,* 421 *Washington Avenue SE, Minneapolis, Minnesota* 55455, *USA*

(Received 11 August 2009; revised manuscript received 28 September 2009)

The product polarizations of the title reactions are investigated by employing the quasi-classical trajectory (QCT) method. The four generalized polarization-dependent differential cross-sections (PDDCSs) $(2\pi/\sigma)(\mathrm{d}\sigma_{00}/\mathrm{d}\omega_t)$, $(2\pi/\sigma)(\mathrm{d}\sigma_{20}/\mathrm{d}\omega_t)$, $(2\pi/\sigma)(\mathrm{d}\sigma_{22+}/\mathrm{d}\omega_t)$, and $(2\pi/\sigma)(\mathrm{d}\sigma_{21-}/\mathrm{d}\omega_t)$ are calculated in the centre-of-mass frame. The distribution of the angle between $\boldsymbol{k}$ and $\boldsymbol{j}'$, $P(\theta_r)$, the distribution of the dihedral angle denoting $\boldsymbol{k}$–$\boldsymbol{k}'$–$\boldsymbol{j}'$ correlation, $P(\phi_r)$, as well as the angular distribution of product rotational vectors in the form of polar plots $P(\theta_r, \phi_r)$ are calculated. The isotope effect is also revealed and primarily attributed to the difference in mass factor between the two title reactions.

Keywords: stereodynamics, quasi-classical trajectory method, vector correlation, polarization-dependent differential cross-section, isotope effect

PACC: 3400, 8200, 8200T

1. Introduction

Molecular dynamics has made exciting progress with the advance in molecular beam and laser spectroscopic techniques, as well as in theoretical methodology and computer capacity in the past decades.[1−8] The key to understanding the elementary reaction dynamics is to ascertain the interaction between state-of-the-art theory and experiments. The quasi-classical trajectory (QCT) method has been verified to be a powerful and popular tool to study the chemical reaction dynamics. Especially for the benchmark three-atom reactions H + H_2,[9] F+H_2,[10] and Cl + H_2,[11] the QCT-calculated results on accurate potential energy surfaces (PESs) are in excellent agreement with quantum ones. Direct abstraction reactions take place in these systems, where there is no potential well on the minimum energy path. In recent years, much attention has been paid to the complex reactions of three atoms which occur on PESs with a deep potential well between reactants and products. $O(^1D)$ + H_2, $C(^1D)$ + H_2, $S(^1D)$ + H_2, and $N(^2D)$ + H_2 reactions belong in this category. These reaction intermediates are the bound species H_2O, H_2C, H_2S, and H_2N, respectively. In particular, considerable theoretical and experimental studies are being carried out currently on the reaction $N(^2D)$ + H_2 and its isotopic variants. This may be due to the important role that the $N(^2D)$ + H_2 reaction plays in the combustion of nitrogen containing fuels and atmospheric chemistry.

It is well known that the accuracy of the theoretical results depends significantly on the accuracy of the PES. Study on the refinement and improvement of the $1^2A''$ PES of NH_2 was conducted recently. Ho *et al.*[12] reported a new reproducing kernel Hilbert space (RKHS) PES for the $1^2A''$ state of NH_2 based on 2715 multireference configuration interaction (MRCI) points. Varandas and Poveda[13] and Qu *et al.*[14] calculated PES for the same system from internally contracted MRCI calculations by using an augmented correlation-consistent polarized valence quadruple zeta (aug-cc-pVQZ) basis set. Based on these accurate PESs, both QM[15−20] and QCT[12,19] calculations have been performed for the $N(^2D)$ + $H_2/D_2/HD$ reactions. Chu *et al.*[16] investigated the reaction probabilities and rate constants of the $N(^2D)$ + H_2 ($\nu = 0$, j=0–5) → NH + H reaction by using the time-dependent quantum wave packet method. Castillo *et al.*[19] investigated the $N(^2D)$ + H_2 ($\nu = 0$, $j = 0$) → NH + H reaction and its D_2 and HD isotopic variants by means of QM real wave packet and

*Project supported by Young Funding of Jining University, China (Grant No. 2009QNKJ02).

†Corresponding author. E-mail: xfyuejnu@gmail.com

© 2010 Chinese Physical Society and IOP Publishing Ltd

wave packet with split operator and QCT methodologies. Rao and Mahapatra[20] calculated the initial state-selected total reaction probabilities, integral cross sections, and thermal rate constants of the N + H_2 reaction. Most of this work[15−20] focused on the calculation of the reaction probability, the integral cross section and the thermal rate constant. The vector properties for the N(^{2}D) + H_2/D_2/HD reactions have been investigated very little. Vector properties, such as velocity and angular momentum, can provide valuable information about chemical reaction stereodynamics.[21] Therefore, it is necessary to study the vector properties for fully understanding the dynamics of the title reactions.

In the present work, we perform QCT calculation of the N(^{2}D) + HD reaction on the accurate 1^2A″ state PES by Ho *et al.*[12] The vector properties in N(^{2}D) + HD → NH + D and ND + H reactions are presented.

2. Theory

2.1. Quasi-classical trajectory calculations

The accurate 1^2A″ state PES constructed recently by Ho *et al.*[12] is employed for the present calculations. The calculation method of QCT is the same as that in Refs. [21]–[24]. The classical Hamilton's equations are numerically integrated in three dimensions. The collision energy is chosen to be 5.1 kcal/mol for the N(^{2}D) + HD reaction. The accuracy of the numerical integration is verified by checking the conservations of the total energy and the total angular momentum for every trajectory. The vibrational and the rotational levels of the reactant molecules are taken to be $\nu = 0$ and $j = 0$, respectively. In the calculation, batches of 10000 trajectories are run for each reaction and the integration step size is chosen to be 0.1 fs. The trajectories start at an initial distance of 15 Å (1 Å=0.1 nm) between the N atom and the centre-of-mass (CM) of the HD molecule. We calculate the reaction probabilities and the integral cross-sections of the N(^{2}D) + H_2/HD/D_2 reactions in the vibrational and rotational ground states. Our calculated results are in good agreement with the previous ones computed by the QCT[12,19] and the exact QM[15] methods under the same PES of Ho *et al.*[12] This confirms that the QCT code, method and PES used in this work are credible for the study of the title reactions.

2.2. Polarization-dependent differential cross-sections (PDDCSs)

The centre-of-mass frame is used as a reference frame in the present work, which is depicted in Fig. 1. The reagent relative velocity vector $\boldsymbol{k}$ is parallel to the z-axis. The x–z plane is the scattering plane which contains the initial and the final relative velocity vectors, $\boldsymbol{k}$ and $\boldsymbol{k}'$. θ_t is the angle between the reagent relative velocity and product relative velocity (so-called scattering angle). θ_r and ϕ_r are the polar and azimuthal angles of the final rotational angular momentum $\boldsymbol{j}'$.

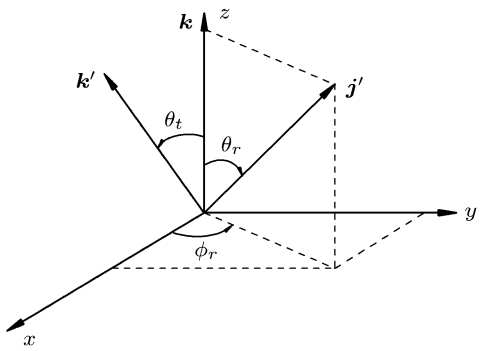


Fig. 1. Centre-of-mass coordinate system used to describe the $\boldsymbol{k}$, $\boldsymbol{k}'$ and $\boldsymbol{j}'$ correlations.

The distribution function $P(\theta_r)$ describing the $\boldsymbol{k}$–$\boldsymbol{j}'$ correlation can be expanded in a series of Legendre polynomials as[25,26]

$$P(\theta_r) = \frac{1}{2}\sum_k (2k+1)a_0^{(k)} P_k(\cos\theta_r), \qquad (1)$$

where

$$\begin{aligned} a_0^{(k)} &= \int_0^{\pi} P(\theta_r) P_k(\cos\theta_r)\sin\theta_r \mathrm{d}\theta_r \\ &= \langle P_k(\cos\theta_r)\rangle. \end{aligned} \qquad (2)$$

The expanding coefficients $a_0^{(k)}$ are called orientation (k is odd) and alignment (k is even) parameters.

The dihedral angle distribution function $P(\phi_r)$ describing $\boldsymbol{k}$–$\boldsymbol{k}'$–$\boldsymbol{j}'$ correlation can be expanded in Fourier series as

$$\begin{aligned} P(\phi_r) = \frac{1}{2\pi}\Bigg(1 + \sum_{\text{even},n\geq 2} a_n \cos n\phi_r\Bigg) \\ + \sum_{\text{odd},n\geq 1} b_n \sin\phi_r, \end{aligned} \qquad (3)$$

where

$$a_n = 2\langle \cos n\phi_r \rangle, \tag{4}$$

$$b_n = 2\langle \sin n\phi_r \rangle. \tag{5}$$

In this calculation, $P(\phi_r)$ is expanded up to $n = 24$, which shows good convergence. The joint probability density function of angles θ_r and ϕ_r, which determine the direction of $\boldsymbol{j}'$, can be written as

$$\begin{aligned} P(\theta_r, \phi_r) &= \frac{1}{4\pi} \sum_{kq} [k] a_q^k C_{kq}(\theta_r, \phi_r)^* \\ &= \frac{1}{4\pi} \sum_{k} \sum_{q \geq 0} [a_{q\pm}^k \cos q\phi_r \\ &\quad - a_{q\mp}^k \sin q\phi_r] C_{kq}(\theta_r, 0). \end{aligned} \tag{6}$$

In this calculation, the polarization parameter is evaluated as

$$a_{q\pm}^k = 2\langle C_{k|q|}(\theta_r, 0) \cos q\phi_r \rangle, \quad k \text{ is even}, \tag{7}$$

$$a_{q\mp}^k = 2\,\mathrm{i}\langle C_{k|q|}(\theta_r, 0) \cos q\phi_r \rangle, \quad k \text{ is odd}. \tag{8}$$

In the calculation, $P(\theta_r, \phi_r)$ is expanded up to $k = 7$, which is sufficient for good convergence.

The full three-dimensional angular distribution associated with $\boldsymbol{k}$–$\boldsymbol{k}'$–$\boldsymbol{j}'$ correlation can be represented by a set of generalized PDDCSs in the CM frame. The fully correlated CM angular distribution is written as[27]

$$P(\omega_t, \omega_r) = \sum_{kq} \frac{[k]}{4\pi} \frac{1}{\sigma} \frac{\mathrm{d}\sigma_{kq}}{\mathrm{d}\omega_t} C_{kq}(\theta_r, \phi_r)^*, \tag{9}$$

where $[k] = 2k + 1$, $(1/\sigma)(\mathrm{d}\sigma_{kq}/\mathrm{d}\omega_t)$ is a generalized polarization-dependent differential cross-section (PDDCS), and $(1/\sigma)(\mathrm{d}\sigma_{kq}/\mathrm{d}\omega_t)$ yields

$$\frac{1}{\sigma} \frac{\mathrm{d}\sigma_{k0}}{\mathrm{d}\omega_t} = 0 \quad (k \quad \text{is odd}), \tag{10}$$

$$\begin{aligned} &\frac{1}{\sigma} \frac{\mathrm{d}\sigma_{kq+}}{\mathrm{d}\omega_t} = \frac{1}{\sigma} \frac{\mathrm{d}\sigma_{kq}}{\mathrm{d}\omega_t} + \frac{1}{\sigma} \frac{\mathrm{d}\sigma_{k-q}}{\mathrm{d}\omega_t} = 0 \\ &(k \text{ even}, \ q \text{ odd or}, \ k \text{ odd}, \ q \text{ even}), \end{aligned} \tag{11}$$

$$\begin{aligned} &\frac{1}{\sigma} \frac{\mathrm{d}\sigma_{kq-}}{\mathrm{d}\omega_t} = \frac{1}{\sigma} \frac{\mathrm{d}\sigma_{kq}}{\mathrm{d}\omega_t} - \frac{1}{\sigma} \frac{\mathrm{d}\sigma_{k-q}}{\mathrm{d}\omega_t} = 0 \\ &(k \text{ even}, \ q \text{ even or}, \ k \text{ odd}, \ q \text{ odd}). \end{aligned} \tag{12}$$

The PDDCS is written in the following form:

$$\frac{1}{\sigma} \frac{d\sigma_{kq\pm}}{\mathrm{d}\omega_t} = \sum_{k_1} \frac{[k_1]}{4\pi} S_{kq\pm}^{k_1} C_{k_1 q}(\theta_t, 0), \tag{13}$$

where the $S_{kq\pm}^{k_1}$ is evaluated by using the expected value expression to be

$$S_{kq\pm}^{k_1} = \langle C_{k_1 q}(\theta_t, 0) C_{kq}(\theta_r, 0) [(-1)^q \mathrm{e}^{\mathrm{i}\,q\phi_r} \pm \mathrm{e}^{-\mathrm{i}\,q\phi_r}] \rangle, \tag{14}$$

where the angular brackets represent an average over all angles. The differential cross-section is given by

$$\frac{1}{\sigma} \frac{\mathrm{d}\sigma_{00}}{\mathrm{d}\omega_t} = P(\omega_t) = \frac{1}{4\pi} \sum_{k_1} [k_1] h_0^{k_1}(k_1, 0) P_{k_1}(\cos\theta_t). \tag{15}$$

The bipolar moments $h_0^{k_1}(k_1, 0)$ are evaluated by using the expectation values of the Legendre moments of the differential cross-section and expressed as

$$S_{00}^{k_1} = h_0^{k_1}(k_1, 0) = \langle P_k(\cos\theta_t) \rangle. \tag{16}$$

The PDDCS with $q = 0$ is presented by

$$\frac{1}{\sigma} \frac{\mathrm{d}\sigma_{k0}}{\mathrm{d}\omega_t} = \frac{1}{4\pi} \sum_{k_1} [k_1] S_{k0}^{k_1} P_{k_1}(\cos\theta_t), \tag{17}$$

where $S_{k0}^{k_1}$ is evaluated by the expected value expression and given as

$$S_{k0}^{k_1} = \langle P_{k_1}(\cos\theta_t) P_k(\cos\theta_r) \rangle. \tag{18}$$

Many photon-initiated bimolecular reaction experiments are sensitive to only those polarization moments with $k = 0$ and $k = 2$. In order to compare calculations with experiments, $(2\pi/\sigma)(\mathrm{d}\sigma_{00}/\mathrm{d}\omega_t)$, $(2\pi/\sigma)(\mathrm{d}\sigma_{20}/\mathrm{d}\omega_t)$, $(2\pi/\sigma)(\mathrm{d}\sigma_{22+}/\mathrm{d}\omega_t)$, and $(2\pi/\sigma)(\mathrm{d}\sigma_{21-}/\mathrm{d}\omega_t)$ are calculated. In the above calculations, PDDCSs are expanded up to $k_1 = 7$, which is sufficient for good convergence.

3. Results and discussion

Figure 2 displays the calculated $P(\theta_r)$ distributions of the N(^{2}D) + HD→ NH + D and N(^{2}D) + HD → ND + H reactions. The product $P(\theta_r)$ distribution describes the $\boldsymbol{k}$–$\boldsymbol{j}'$ correlation. It is clear that the peak of the $P(\theta_r)$ distribution is at $\theta_r = 90°$, and the $P(\theta_r)$ distribution is symmetric with respect to 90°. This indicates that the product rotational angular momentum vector ($\boldsymbol{j}'$) is strongly aligned along the direction at right angles to the relative velocity direction ($\boldsymbol{k}$). Obviously, the $P(\theta_r)$ distributions are different for the two title reactions. The peak of $P(\theta_r)$ distribution for the reaction N(^{2}D) + HD → ND + H is higher than that of the reaction N(^{2}D) + HD → NH + D, which indicates that the degree of alignment of the ND product is stronger than that of NH. According to Ref. [28], the $P(\theta_r)$ is sensitive to two factors: one is the character of PES, and the other is the mass factor (i.e. $\cos^2\beta = m_\mathrm{A} m_\mathrm{B}/(m_\mathrm{A} + m_\mathrm{B})(m_\mathrm{B} + m_\mathrm{C})$

for the reaction A + BC → AB + C). In our calculation, the same PES is used for both title reactions. Therefore, the difference between $P(\theta_r)$ distributions is probably attributed to the difference in mass factor between the reaction N(^{2}D) + HD → NH + D ($\cos^2\beta = 0.311$) and the reaction N(^{2}D) + HD → ND + H ($\cos^2\beta = 0.583$).

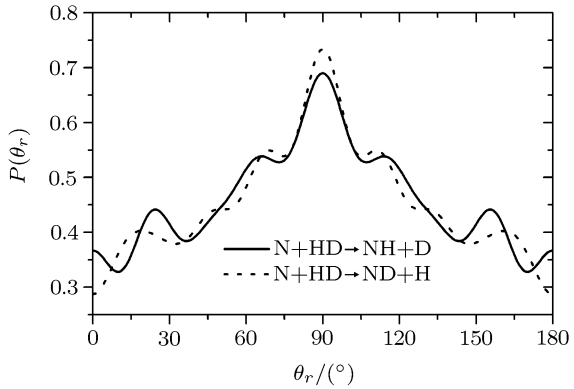


Fig. 2. Angular distributions of $P(\theta_r)$ describing the $\boldsymbol{k}$–$\boldsymbol{j}'$ correlation.

The dihedral angle distributions $P(\phi_r)$ describing the $\boldsymbol{k}$–$\boldsymbol{k}'$–$\boldsymbol{j}'$ correlations are depicted in Fig. 3. As shown in Fig. 3, the $P(\phi_r)$ distributions tend to be asymmetric with respect to the $\boldsymbol{k}$–$\boldsymbol{k}'$ scattering plane (or at about $\phi_r = 180°$), which reflects the strong polarization of the product angular momenta in the two title reactions. The peaks of the $P(\phi_r)$ distributions appear only at $\phi_r = 270°$, which means that the rotational angular momentum vectors of the NH and ND products from the two reactions are oriented along the negative direction of y-axis. It can be obviously seen from Fig. 3 that the orientation of the NH product from the N(^{2}D) + HD→ NH + D reaction is almost the same as that of the ND product from the N(^{2}D) + HD → ND + H reaction.

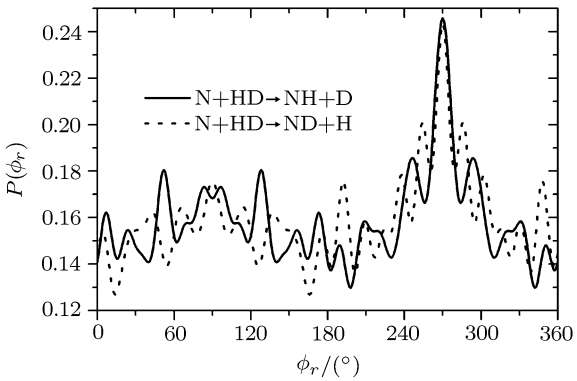


Fig. 3. Dihedral angle distributions of $\boldsymbol{j}'$ with respect to the $\boldsymbol{k}$–$\boldsymbol{k}'$ plane.

It seems interesting that the title reactions are symmetric about the relative velocity vector, while the distribution of $P(\phi_r)$ is asymmetric. According to the previous benchmark study about the impulsive model of the atom and molecule reaction for the reaction A + BC → AB + C,[29,30] we have $\boldsymbol{j}' = \boldsymbol{L}\sin^2\beta + \boldsymbol{j}\cos^2\beta + \boldsymbol{J}_1 m_{\rm B}/m_{\rm AB}$, where $\boldsymbol{L}$ is the reagent orbital angular momentum, $\boldsymbol{J}_1 = \sqrt{\mu_{\rm BC}R}(\boldsymbol{r}_{\rm AB} \times \boldsymbol{r}_{\rm CB})$, with $\boldsymbol{r}_{\rm AB}$ and $\boldsymbol{r}_{\rm CB}$ being the unit vectors and B pointing to A and C, respectively, $\mu_{\rm BC}$ is the reduced mass of the BC molecule and R is the repulsive energy between B and C atoms. During the chemical bond forming and breaking for the reaction N(^{2}D) + HD→ NH + D or N(^{2}D) + HD → ND + H, the term $\boldsymbol{L}\sin^2\beta + \boldsymbol{j}\cos^2\beta$ in the equation is symmetric, while the term $\boldsymbol{J}_1 m_{\rm B}/m_{\rm AB}$ shows a preferable direction because of the effect of the repulsive energy, which leads to the orientation of the products NH or ND.

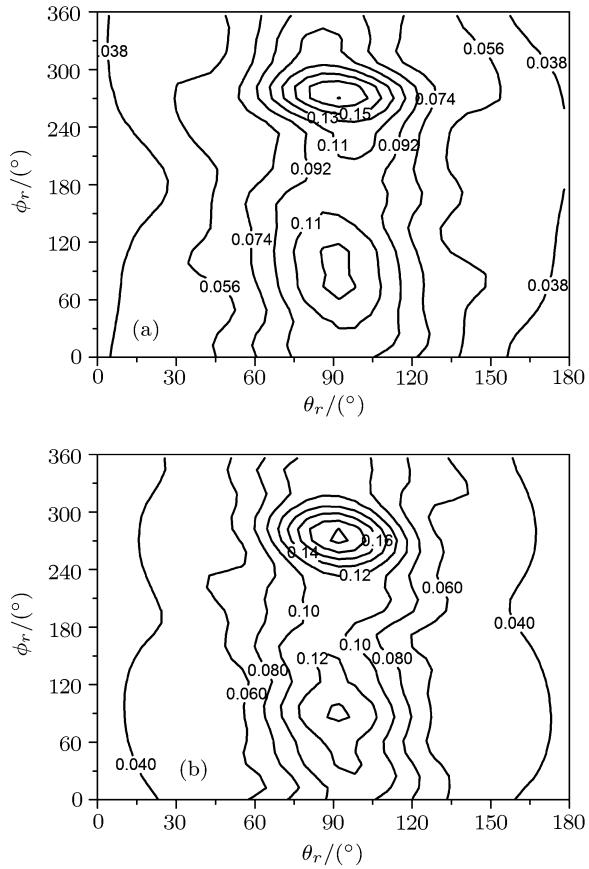


Fig. 4. (a) Polar plots of $P(\theta_r, \phi_r)$ distribution averaged over all scattering angles for the N(^{2}D) + HD→ NH + D reaction, and (b) the same as (a) but for the N(^{2}D) + HD → ND + H reaction.

In order to validate more information about the angular momentum polarization, we plot it in the form of poplar plots θ_r and ϕ_r averaged over all scattering angles in Fig. 4. As shown in Fig. 4, the $P(\theta_r, \phi_r)$

distributions peak at (90°, 270°) for both NH and ND products from the two reactions, which are in good accordance with the $P(\theta_r)$ and $P(\phi_r)$ distributions mentioned above. The $P(\theta_r, \phi_r)$ distributions displayed in Fig. 4 indicate that the NH and ND products are strongly polarized in the direction perpendicular to the scattering plane and mainly rotating in planes parallel to the scattering plane.

The generalized PDDCSs describe the $\boldsymbol{k}$–$\boldsymbol{k}'$–$\boldsymbol{j}'$ correlation and the scattering direction of the product molecule. The calculated results of the PDDCSs for the N(^{2}D) + HD→ NH + D and N(^{2}D) + HD → ND + H reactions are shown in Fig. 5. The PDDCS $(2\pi/\sigma)(\mathrm{d}\sigma_{00}/\mathrm{d}\omega_t)$ is simply proportional to the differential cross-section (DCS), and only describes the $\boldsymbol{k}$–$\boldsymbol{k}'$ correlation or the product angular distributions. Figure 5(a) displays the $(2\pi/\sigma)(\mathrm{d}\sigma_{00}/\mathrm{d}\omega_t)$ results of the NH and the ND products from the N(^{2}D) + HD→ NH + D reaction and the N(^{2}D) + HD → ND + H reaction, respectively. As clearly shown in Fig. 5(a), the ND product angular distributions are nearly backward–forward symmetric for the N(^{2}D) + HD → ND + H reaction. The NH product angular distributions are slightly away from the backward–forward symmetry, but peak in backward bias. The characteristics of these product angular distributions reflect an insertion dynamics for the title reactions.

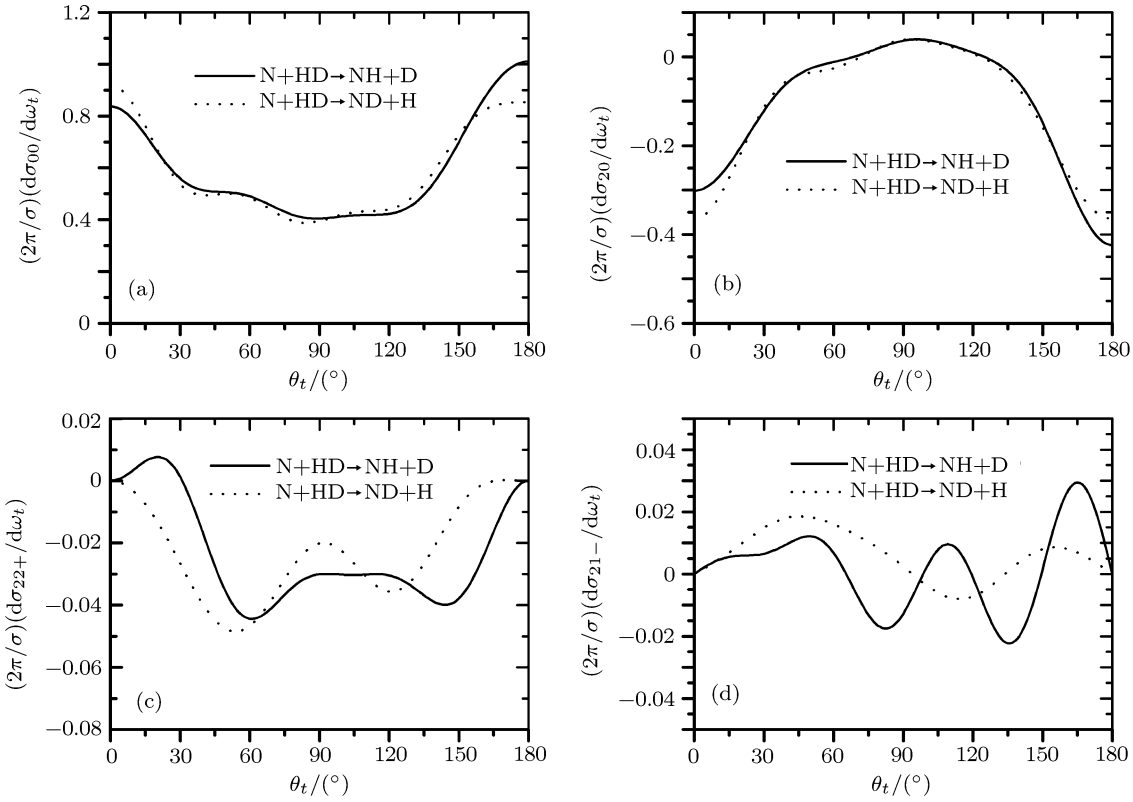


Fig. 5. PDDCSs with $(k, q) = (0, 0)$ (a) and $(2, 0)$ (b) and with $(k, q\pm) = (2, 2+)$ (c) and $(2, 1-)$ (d).

The PDDCS $(2\pi/\sigma)(\mathrm{d}\sigma_{20}/\mathrm{d}\omega_t)$ is the expectation value of the second Legendre moment $\langle P_2(\cos\theta_r)\rangle$ and contains the alignment information of $\boldsymbol{j}'$ with respect to $\boldsymbol{k}$. As shown in Fig. 5(b), the behaviour of the $(2\pi/\sigma)(\mathrm{d}\sigma_{20}/\mathrm{d}\omega_t)$ distribution demonstrates an opposite trend to that the $(2\pi/\sigma)(\mathrm{d}\sigma_{00}/\mathrm{d}\omega_t)$ and obviously depends on scattering angle θ_t. It can be clearly seen from Fig. 5(b) that the $(2\pi/\sigma)(\mathrm{d}\sigma_{20}/\mathrm{d}\omega_t)$ values of the two title reactions are negative for both backward and forward scatterings, but they are close to zero for sideways scattering. These results suggest that the $\boldsymbol{j}'$ polarizes preferentially along the direction perpendicular to $\boldsymbol{k}$ when the products are scattered forward and backward. In addition, the average values of the second Legendre moment $\langle P_2(\cos\theta_r)\rangle$ are calculated and found to be −0.360 and −0.389 corresponding to N(^{2}D) + HD→ NH + D and N(^{2}D) + HD → ND + H reactions respectively, which indicates the product rotational alignment of ND is stronger than that of NH. This is consistent with the product alignment prediction from the $P(\theta_r)$ distribution shown in Fig. 2.

Figures 5(c) and 5(d) illustrate the PDDCSs distributions with $q \neq 0$. All of the PDDCSs with $q \neq 0$ are equal to zero at the extremities of forward and backward scatterings. The $(2\pi/\sigma)(\mathrm{d}\sigma_{22+}/\mathrm{d}\omega_t)$ value is positive or negative depending on the preference of $\boldsymbol{j}'$ alignment along the x axis or y axis. It can be seen from Fig. 5(c) that the $(2\pi/\sigma)(\mathrm{d}\sigma_{22+}/\mathrm{d}\omega_t)$ values of the N(^{2}D) + HD $\rightarrow$ ND + H reaction is negative for all scattering angles, which indicates that the alignments of the ND products prefer to be along the y axis. However, for the N(^{2}D) + HD $\rightarrow$ NH + D reaction, the $(2\pi/\sigma)(\mathrm{d}\sigma_{22+}/\mathrm{d}\omega_t)$ values are slightly positive at the scattering angles below about 30°, but they are negative at other scattering angles. This indicates that the alignments of the NH product are along both the x axis and the y axis, but primarily along the y axis. The $(2\pi/\sigma)(\mathrm{d}\sigma_{22+}/\mathrm{d}\omega_t)$ distribution of the N(^{2}D) + HD $\rightarrow$ NH + D reaction displays a stronger polarization at about 60° and 150°. Nevertheless, the $(2\pi/\sigma)(\mathrm{d}\sigma_{22+}/\mathrm{d}\omega_t)$ displays a stronger polarization at about 50° and 120° for the N(^{2}D) + HD $\rightarrow$ ND + H reaction. The PDDCS $(2\pi/\sigma)(\mathrm{d}\sigma_{21-}/\mathrm{d}\omega_t)$ is related to $\langle \sin^2\theta_r \cos 2\phi_r \rangle$ and its distribution is depicted in Fig. 5(d). As shown in Fig. 5(d), the $(2\pi/\sigma)(\mathrm{d}\sigma_{21-}/\mathrm{d}\omega_t)$ distribution shows a strongest polarization separately at about $\theta_t = 80°$, 135°, 165° for the N(^{2}D) + HD $\rightarrow$ NH + D reaction. Correspondingly, the $(2\pi/\sigma)(\mathrm{d}\sigma_{21-}/\mathrm{d}\omega_t)$ distribution shows a strongest polarization at about $\theta_t = 45°$ for the N(^{2}D) + HD $\rightarrow$ ND + H reaction. These results indicate that the product angular distributions are anisotropic for both the N(^{2}D) + HD $\rightarrow$ NH + D and N(^{2}D) + HD $\rightarrow$ ND + H reactions.

4. Conclusions

This paper presents a quasi-classical trajectory study on the product polarization for the reactions N(^{2}D) + HD $\rightarrow$ NH + D and N(^{2}D) + HD $\rightarrow$ ND + H at a collision energy of 5.1 kcal/mol. Four PDDCSs and the distributions of $P(\theta_r)$, $P(\phi_r)$, and $P(\theta_r, \phi_r)$ have been calculated. The results demonstrate that the angular distributions of NH and ND products are in both forward and backward scatterings. The degree of alignment of the ND product is stronger than that of the NH, but the degrees of orientation of the two products are almost the same. The pronounced isotope effect is also revealed and primarily attributed to the difference in mass factor between the two title reactions.

References

[1] Han K L and He G Z 2007 *J. Photochem. Photobiol.* C: *Photochem. Rev.* **8** 55
[2] Liu Y F, Jiang L J, Ma H and Sun J F 2008 *Chin. Phys.* B **17** 1674
[3] Chu T S, Zhang Y and Han K L 2006 *Int. Rev. Phys. Chem.* **25** 201
[4] Yan S, Wu Y T, Zhang B, Yue X F and Liu K P 2007 *Science* **316** 1723
[5] Yue X F, Sun J L, Yin H M, Wei Q and Han K L 2009 *J. Phys. Chem.* A **113** 3303
[6] Shi D H, Zhang J P, Sun J F, Liu Y F, Zhu Z L, Ma H and Yang X D 2008 *Chin. Phys.* B **17** 3678
[7] Luo W L, Ruan W, Zhang L, Zhu Z H and Fu Y B 2009 *Chin. Phys.* B **18** 167
[8] Chi B Q, Liu L and Wang J G 2008 *Chin. Phys.* B **17** 2890
[9] Chu T S and Han K L 2008 *Phys. Chem. Chem. Phys.* **10** 2431
[10] Chen M D, Han K L and Lou N Q 2002 *Chem. Phys. Lett.* **357** 483
[11] Chen M D, Han K L and Lou N Q 2003 *J. Chem. Phys.* **118** 4463
[12] Ho T S, Rabitz H, Aoiz F J, Bañares L, Vázquez S A and Harding L B 2003 *J. Chem. Phys.* **119** 3063
[13] Varandas A J C and Poveda L A 2006 *Theor. Chem. Acc.* **116** 4
[14] Qu Z W, Zhu H, Schinke R, Adam L and Hack W 2005 *J. Chem. Phys.* **122** 204313
[15] Lin S Y and Guo H 2006 *J. Chem. Phys.* **124** 031101
[16] Chu T S, Han K L and Varandas A J C 2006 *J. Phys. Chem.* A **110** 1666
[17] Varandas A J C, Chu T S, Han K L and Caridade P J S B 2006 *Chem. Phys. Lett.* **421** 415
[18] Chu T S, Duan Y B, Yuan S P and Varandas 2007 *Chem. Phys. Lett.* **444** 351
[19] Castillo J F, Bulut N, Bañares L and Gogtas F 2007 *Chem. Phys.* **332** 119
[20] Rao B J and Mahapatra S 2007 *J. Chem. Phys.* **127** 244307
[21] Han K L, He G Z and Lou N Q 1996 *J. Chem. Phys.* **105** 8699
[22] Zhang X and Han K L 2006 *Int. J. Quantun Chem.* **106** 1815
[23] Han K L, Zhang L, Xu D L, He G Z and Lou N Q 2001 *J. Phys. Chem.* A **105** 2956
[24] Xu W W, Liu X G, Luan S X, Sun S S and Zhang Q G 2009 *Chin. Phys.* B **18** 339
[25] Chen M D, Han K L and Lou N Q 2002 *Chem. Phys.* **283** 463
[26] Ma J J, Chen M D, Cong S L and Han K L 2006 *Chem. Phys.* **327** 529
[27] Wang M L, Han K L and He G Z 1998 *J. Chem. Phys.* **109** 5446
[28] Wang M L, Han K L and He G Z 1998 *J. Phys. Chem.* A **102** 20204
[29] Chen M D, Han K L and Lou N Q 2002 *Chem. Phys. Lett.* **357** 483
[30] Li R J, Han K L, Li F E, Lu R C, He G Z and Lou N Q 1994 *Chem. Phys. Lett.* **220** 281